

Hotspots of recent drought in Asian steppes

Masato Shinoda · Banzragch Nandintsetseg ·
Urianhai Galzuud Nachinshonhor · Hiroshi Komiyama

Received: 22 November 2012 / Accepted: 16 April 2013 / Published online: 8 May 2013
© The Author(s) 2013. This article is published with open access at Springerlink.com

Abstract The present study aims to identify hotspots on the Asian steppe that were vulnerable to widespread drought events in the Northern Hemisphere during 1999–2002, using newly proposed indices of vegetation response (sensitivity and resilience) to drought. Drought sensitivity is defined as vegetation response to decreased precipitation from pre-drought to drought phases, and resilience is defined as response to increased precipitation from drought to post-drought phases. Thus, the sensitivity and resiliency indices SI and RI are similarly expressed as normalized change of vegetation relative to that of precipitation. We also develop new regionally adjusted indices SI_r and RI_r , to do an interregional comparison of vegetation dynamics. In general, the resilience (RI_r or RI) was larger than sensitivity (SI_r or SI) over the entire region, whereas they had similar amplitudes over a wetter region (forest steppe). This asymmetric response of $SI_r < RI_r$, which manifested over the desert steppe/steppe regions, is

explained by interannual change of plant species composition (i.e., larger ratio of annual/perennial species for the post-drought year of 2003). As for the steppe region, the Chinese section had much higher resilience during the post-drought year compared with the Mongolian one. This may be attributable to the larger annual/perennial ratio, but is not strongly related to grazing pressure. Spatial and temporal analyses of the indices identified locations where there was not resilience from drought-affected vegetation conditions despite increased precipitation, and/or where long-term stability of vegetation is under threat.

Keywords Drought · Vulnerability · Sensitivity · Resilience · Steppe · NDVI

Introduction

The new field of sustainability science has emerged since the late 1990s (e.g., Kates et al. 2001; Clark and Dickson 2003). Since then, continuous efforts have been made to develop a conceptual framework for characterizing vulnerability (e.g., Turner et al. 2003; Füssel 2007). For example, in climate change studies, vulnerability is defined as the degree to which a system is susceptible to, and unable to cope with, adverse effects of climate change, including climate variability and extremes (IPCC 2007). Herein, vulnerability is a function of the character, magnitude, and rate of climate change and variation to which a system is exposed, its sensitivity and adaptive capacity. Given this background, the present paper develops a method to systematically measure the degree of ecosystem vulnerability to climate change (especially drought) on the continental scale. In general, vulnerability is considered to comprise three components, namely exposure, sensitivity,

M. Shinoda (✉)
Arid Land Research Center, Tottori University, 1390, Hamasaka,
Tottori 680-0001, Japan
e-mail: shinoda@alrc.tottori-u.ac.jp

B. Nandintsetseg
Institute of Meteorology, Hydrology and Environment,
Juilchny gudamj-5, Ulaanbaatar 210646, Mongolia
e-mail: nandiad98@gmail.com

U. G. Nachinshonhor
Graduate School of Environmental and Life Science,
Okayama University, Okayama 700-8530, Japan
e-mail: galzuud@gmail.com

H. Komiyama
Japan International Research Center for Agricultural Sciences,
Tsukuba 305-8686, Japan
e-mail: komiyam@affrc.go.jp

and resilience. This analysis defines the combination of the latter two components for a region as forming its vulnerability. This is because there is no strategy for eliminating exposure of regional vegetation to unusual weather by measures such as moving its location on a yearly basis, as with animals.

Drought has been identified as the most hazardous natural disaster worldwide, in terms of numbers of humans killed and/or adversely affected (Obasi 1994; Guha-Sapir et al. 2004). Drought impacts are non-structural and spread over a larger geographic area than are damages from other natural hazards (Wilhite 2000). A steep drying trend has been observed in soil moisture index values over Northern Hemisphere land areas since the mid-1950s, especially across northern Africa, Canada, Alaska, and Eurasia, including Mongolia (Dai et al. 2004; Nandintsetseg and Shinoda 2012). In particular, below-normal precipitation in the Northern Hemisphere during 1999–2002 appears to have extensively decreased vegetation activity over Eurasia and North America, as revealed by the satellite-estimated normalized difference vegetation index (NDVI) (Lotsch et al. 2005). The present work focuses on the 4-year, below-normal precipitation period of 1999–2002. It was the most pronounced on the hemispheric scale of the multiyear droughts during the past several decades. Global synthesis reveals that the greatest documented effect on primary production among various environmental changes (e.g., ultraviolet radiation, acidification) was from drought, which was comparable to species loss exceeding that of prior mass extinctions ($\geq 75\%$) (Hooper et al. 2012). However, these changes are unlikely to occur globally.

In Mongolia, the growing drought frequency has had increasingly important effects on animal husbandry and pasturing (e.g., Natsgadorj 2003; Nandintsetseg and Shinoda 2013). The effects of drought on Mongolian grasslands have been both quantitative, such as decreases in aboveground phytomass (AGP) (Miyazaki et al. 2004; Zhang et al. 2005; Munkhtsetseg et al. 2007), and qualitative, such as changes in phenology (Kondoh et al. 2005; Shinoda et al. 2007) and species composition combined with grazing intensity (Fernandez-Gimenez and Allen-Diaz 1999, 2001; Sasaki et al. 2009; Wesche et al. 2010; Cheng et al. 2011). Drought and grazing always interact to affect ecosystem processes in grazed grasslands (Milchunas et al. 1989; Hartvigsen 2000).

For China as a whole, there were no long-term trends in percentage areas of soil moisture droughts (defined as Palmer drought severity index < -1.0) from 1951 to 2003 (Zou et al. 2005). However, increases in drought areas were found in much of northern China (but not in Northwest China), aggravated by warming and decreasing precipitation (Ma and Fu 2003; Wang and Zhai 2003), consistent with Dai et al. (2004). As for Inner Mongolia, a

precipitation deficit from 1999 to 2001 or 2002 reduced the NDVI for various vegetation types (Chuai et al. 2012). Severe drought combined with heavy grazing (≥ 4 sheep/ha) in Inner Mongolia has greatly altered species composition and functional components, degrading perennial grasslands in conjunction with increased proportions of annual species (Gao et al. 2009).

We carried out the drought experiment DREX (Shinoda et al. 2010) to examine drought impacts on dryland systems. DREX was designed to examine the direction of ecosystem response to a severe drought with return interval 60–80 years, which was simulated using a rainout shelter on the Mongolian steppe during a rainy season. The drought drastically reduced AGP and soil water, but did not substantially affect belowground phytomass (BGP). AGP in a drought plot quickly approached that in a control plot by late summer (August) of the first post-drought year, likely because BGP (which was several times AGP) was not as severely damaged by the drought. Despite the drought intensity, a large root system provided a basis for quick resilience of AGP without a shift to a drier equilibrium community. We also developed the sensitivity and resiliency indices *SI* and *RI* to quantify vegetation response to drought.

Given results from this field experiment, we extended the plot-scale analysis to a larger (continental) scale, using remote sensing data. That experiment was conducted in a fenced plot that prevented grazing, but human impacts on the land increased relative to the pre-industrial period (de Noblet-Ducoudré et al. 2012). This trend was dominant in eastern Inner Mongolia and Northeast China, generally coinciding with the pattern of desertification (UNEP 1992) and a land-cover change from 1981 to 2000 (Lepers et al. 2005). Given this background, satellite remotely sensed data offer considerable advantages, such as in exploring spatiotemporal drought evolution with consistent spatial resolution and homogeneity. Previous studies developed a variety of drought indices from remote sensing, which were applied to Mongolia and China (e.g., Chen et al. 1994; Bayarjargal et al. 2006). Also, high correlation between rainfall and time-lagging NDVI during the growing season was documented (e.g., Wang et al. 2002; Iwasaki 2006; Nandintsetseg et al. 2010). However, only a few studies applied NDVI in sensitivity and resilience analyses on the continental scale (e.g., Vicente-Serrano et al. 2012). To our knowledge, this is the first attempt to measure vegetation vulnerability using the $\Delta\text{NDVI}/\Delta\text{Precipitation}$ ratio (i.e., rate of interannual NDVI change relative to that of precipitation) as an index of sensitivity and resilience (as given by Eqs. 1, 2). The concept here is analogous to that of conventional sensitivity analysis, which is used to ascertain how a given system output (e.g., internal state of vegetation) depends upon input parameter(s) (e.g., external forcing of precipitation). In this study, “sensitivity” to drought is

defined as vegetation response to decreased precipitation from pre-drought to drought phases, and “resilience” to drought is defined as its response to increased precipitation from drought to post-drought phases; taken together, they represent a measure of “vulnerability.”

This study is designed to address the following questions: (1) How did vegetation respond to the drought event in terms of the sensitivity and resilience indices? (2) How did the responses (as revealed by both indices) vary regionally? (3) How were the responses related to vegetation dynamics and human activities? (4) How are the vulnerability and instability of regional vegetation measured by the indices?

Methods

General approach

First, we analyzed spatial patterns of interannual changes of precipitation and NDVI to examine whether the 1999–2002 drought was sufficiently widespread to cover the entire study area (Asian steppe) (Fig. 3). Second, we conducted time-series analysis of precipitation and NDVI for different vegetation regions in the study area, to investigate how coherently they varied on a yearly basis (Fig. 4). Third, we used two types of sensitivity and resiliency indices as calculated from the time-series data, to explore how regional vegetation responded to the drought event (Figs. 5, 6, 7). Fourth, we combined information of the two indices to identify vulnerability and instability hotspots (Figs. 8, 9). Finally, we related the drought responses to vegetation dynamics, as indicated by species composition (Fig. 10), land-use management (Fig. 11), and grazing pressure (Fig. 12).

Formulating sensitivity and resiliency indices

In the present study, the new drought sensitivity and resiliency indices developed by Shinoda et al. (2010) were applied in analyses of precipitation and NDVI change on the Asian steppe to measure ecosystem vulnerability. Tilman and Downing (1994) proposed the relative rate of phytomass change (dM/Mdt , year^{-1}) between pre-drought and drought years as a means for quantifying sensitivity (or in the opposite sense, resistance) of a plant community to drought. In this parameter, M denotes AGP in the pre-drought year. Shinoda et al. (2010) modified this index by replacing M with the multiyear average M_m , and by considering quantitative effects of precipitation change (dP/P_mdt , year^{-1}), which have the strongest influence on the phytomass of drylands, all else being equal. The resulting sensitivity index (SI) is thus

$$SI = \frac{dM_{\text{pre}}/dP_{\text{pre}}}{M_m/P_m} \quad (1)$$

where dM_{pre} and dP_{pre} denote changes from the pre-drought to drought year of phytomass and precipitation, respectively; M_m and P_m represent multiyear averages of phytomass and precipitation, respectively. The resilience index (RI) can be expressed similarly:

$$RI = \frac{dM_{\text{post}}/dP_{\text{post}}}{M_m/P_m} \quad (2)$$

where dM_{post} and dP_{post} symbolize changes from the drought to post-drought year of phytomass and precipitation, respectively. The value of M_m/P_m corresponds to the climatological, site-specific rain-use efficiency (Huxman et al. 2004), if we assume that AGP is a good approximation of warm-season, aboveground net primary production for the grassland ecosystem. The advantage of these indices relative to those used by Tilman and Downing (1994) and Bai et al. (2004) is as follows. With the addition of M_m/P_m , we can compare ecosystem sensitivity and resilience with those of other regions. The normalizing procedure from addition of this parameter is necessary because values of $dM_{\text{pre}}/dP_{\text{pre}}$ and $dM_{\text{post}}/dP_{\text{post}}$ vary by region, depending on the degree of aridity. A similar concept was developed for climate sensitivity to an external forcing (e.g., Schneider and Dickinson 1974; Charney et al. 1979), and has been widely used in recent climate change studies. These dealt with the “equilibrium” state of the system, but we did not.

In the present large-scale analysis, the NDVI value was used, instead of the AGP in the site-scale analysis (Shinoda et al. 2010). Figure 1 illustrates how to derive parameters in the time series that are used in calculation of the indices. Given the hemispheric-scale drought during 1999–2002, we calculated $dNDVI_{\text{pre}}/dP_{\text{pre}}$ using data between 1998 and 1999, and $dNDVI_{\text{post}}/dP_{\text{post}}$ with data between 2002 and 2003.

Moreover, regionally adjusted indices of sensitivity (SI_r) and resilience (RI_r) of vegetation to drought were used to do an interregional comparison of interannual vegetation dynamics, because regional averages (AVE) of SI and RI (solid lines in Fig. 7) vary substantially by region and have decreasing trends for a wetter climate. When the two indices equal (or are larger/smaller than) one, rates of those changes are the same as (or are larger/smaller than) the regional climatology, which is useful for measuring year-to-year dynamics.

Vulnerability and instability analyses

Continental-scale analysis of SI and RI vectors was performed, that is, $S(dP_{\text{pre}}/P_m, dNDVI_{\text{pre}}/NDVI_m)$ and

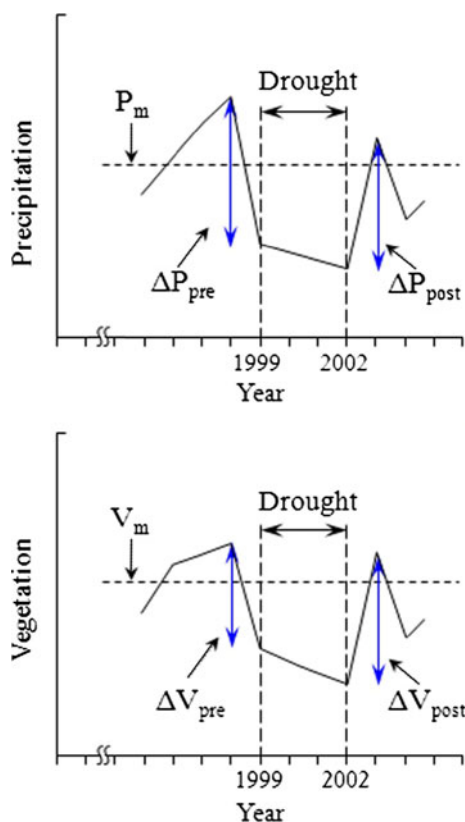


Fig. 1 Schematic yearly time series of P_{6-8} (mm) and $NDVI_8$, and parameters used for calculation of sensitivity and resilience indices for drought event of 1999–2002 (see Eqs. 1, 2)

$R(dP_{post}/P_m, dNDVI_{post}/NDVI_m)$, to detect vulnerability hotspots. Non-resilient areas were identified as those where composite vectors of $R + S$ indicated decreased vegetation despite increased precipitation during the post-drought year (indicated by red vector with southeastward direction in Fig. 8). Highly resilient areas were where the $R + S$ vectors indicated increased vegetation despite decreased precipitation in the post-drought year (indicated by blue vector with northwestward direction).

Moreover, trend analysis was done for SI and RI over the past three decades, to investigate the instability of vegetation under a changing climate (Fig. 9). Values of SI and RI with negative signs were not used (not plotted in Fig. 9), as they were in Fig. 3. Values of SI (or RI) with dP_{pre}/P_m (or dP_{post}/P_m) < 0.1 (10 %) were also not used, to exclude extremely high values that might have an unexpectedly large effect on the trend analysis.

Data acquisition and processing

Precipitation data

We used monthly precipitation data from the high-resolution climate gridded dataset CRU TS 3.1 (available at

http://badc.nerc.ac.uk/view/badc.nerc.ac.uk__ATOM__dataent_1256223773328276), which was produced at the Climatic Research Unit (CRU) of the University of East Anglia (Mitchell and Jones 2005; CRU 2012). This database includes nine climate variables for the period 1901–2009 and extends over the global land surface at 0.5° spatial resolution. The database is checked for inhomogeneities in station records, using an automated method that refines previous methods. This is done using incomplete and partially overlapping records, and by detecting inhomogeneities of opposite signs in different seasons.

NDVI data

We used a monthly $0.5^\circ \times 0.5^\circ$ NDVI data grid from Global Inventory Modeling and Mapping Studies (GIMMS) for the period 1982–2006, and moderate resolution imaging spectroradiometer (MODIS) data from 2007 to 2009. We derived a 21-year (1982–2002) monthly $0.5^\circ \times 0.5^\circ$ grid of NDVI data from the semimonthly 8-km resolution GIMMS dataset, produced by Tucker et al. (2005). For 2003–2006, we derived monthly $0.5^\circ \times 0.5^\circ$ NDVI data grids from the semimonthly 8-km resolution GIMMS data, by taking the mean of the two semimonthly data. The GIMMS NDVI datasets were generated from National Oceanic and Atmospheric Administration/Advanced Very High Resolution Radiometer (NOAA/AVHRR) data, which include corrections for NDVI variations from calibration, view geometry, volcanic aerosols, and other factors unrelated to vegetation change (Pinzon 2002; Tucker et al. 2005). For 2007–2009, we derived monthly $0.5^\circ \times 0.5^\circ$ grids of NDVI data from the 16-day $0.05^\circ \times 0.05^\circ$ spatial resolution Global MOD13C1 dataset, obtained from the NASA Land Processes Distributed Active Archive Center (LP DAAC). MODIS NDVI data complement NOAA/AVHRR NDVI products and provide continuity for historical applications (Tucker et al. 2005; Brown et al. 2006; LP DAAC 2012). The MODIS NDVI product contains atmospherically corrected, bi-directional surface reflectances masked for water, clouds, and cloud shadows. In the present study, precipitation (P) for June–August (P_{6-8}) and NDVI for August ($NDVI_8$) were analyzed, because they are the most highly correlated. This is because we focused on water-controlled ecosystems (Nemani et al. 2003) in the Asian interior of the arid region defined by UNEP (1992). Temperature was not significantly correlated with NDVI in the study area during summer (not shown).

Ground-based vegetation data

AGP data from ecological observing site BU_s ($46^\circ 49' 47.46''N$, $105^\circ 47' 35.34''E$, 1,354 masl) were used,

because they cover a long-term continuous period during and after the 1999–2002 drought (Nachinshonhor 2012). This site is approximately 30 km southwest of the Bayan Unjuul DREX site (47°0′37.2″N, 105°57′04.9″E, 1,200 masl) (Shinoda et al. 2010). Both sites are characterized by a semi-arid climate, defined on the basis of an aridity index (UNEP 1992) between 0.20 and 0.50 and steppe vegetation (Yunatov 1976). Meteorological observations approximately 400 m southeast of the DREX site center were made by an Institute of Meteorology, Hydrology and Environment of Mongolia (IMHE) monitoring station. Data from the IMHE station reveal that annual precipitation during 1995–2005 averaged 163.0 mm and concentrated in the summer months of May–August (124.4 mm). Annual mean temperature was 0.1 °C, with a maximum 20.6 °C in July and minimum –24.0 °C in January. Soil was frozen during the 6-month winter (October–March). We analyzed data of plant-available precipitation at IMHE from 1 May to the previous dates of phytomass sampling in August or September, because this period generally coincides with that of plant growth in the Mongolian grasslands (Shinoda et al. 2007).

The vegetation is co-dominated by monocotyledons (*Agropyron cristatum* and *Stipa krylovii*), perennial dicotyledons (*Artemisia adamsii*), annual dicotyledons (*Chenopodium* spp.), and shrubs (*Caragana* spp.) (Nachinshonhor 2012). The ratio of annual to perennial phytomass (Ann/Per) was used in the analysis of species composition. This ratio is a simple but commonly used indicator to represent general composition of functional groups. Herein, functional group is a category composed of plant species that perform mostly the same type of function in the ecosystem.

Livestock data

We performed a sub-regional analysis of relationships between precipitation, NDVI, and land use. The five sub-regions were defined along cross sections 104.75–106.25°E and 43.25–45.75°N, as the desert steppe (DS_m), Mongolian (S_m) and Chinese (S_c) steppes, Mongolian forest steppe (FS_m), and Chinese agro-pastoral region (A_c). These sub-regions were defined so that they coincided roughly with the natural vegetation types of Mongolia (Yunatov 1976) and China (China Vegetation Atlas Editorial Committee, CAS 2001) (Table 1). In addition, S_m and S_c were established so that they had similar climatological precipitation and NDVI conditions. DS_m includes two square areas on the desert steppe. All sub-regions were identified as available for the present analysis according to criteria explained below (Fig. 3).

Land use includes pasturing and cultivation. Data of livestock number at the county (*soum*) level of Mongolia

from 1990 to 1995 were obtained from *Agriculture in Mongolia 1971–1995, A Statistical Profile*, and those from 1996 to 2009 acquired directly from the National Statistical Office of Mongolia. Data for Inner Mongolia were obtained from *The Inner Mongolia Statistical Yearbook*. Livestock number was measured at the end of the year (December).

Livestock numbers for each sub-region were converted into a sheep unit (Su). Conversion rates to Su are as follows. In Mongolia, 1 camel = 5 Su, 1 horse = 7 Su, 1 cattle = 6 Su, 1 sheep = 1 Su, and 1 goat = 0.9 Su; in Inner Mongolia, 1 large animal = 6 Su, and 1 sheep or goat = 1 Su. Livestock density was calculated by dividing livestock number (Su) by area (hectare). A_c is characterized by the Northeast China area in transition from the pastoral region in the northwest to the agricultural region in the southeast. Sub-regional values of livestock density were calculated by averaging data from smaller administrative units (*soum* in Mongolia or banner in China).

Results and discussion

Figure 2 depicts patterns of annual mean precipitation and NDVI for August (1981–2009) across the study area and sub-regions, the desert steppe (DS_m), Mongolian (S_m) and Chinese (S_c) steppes, Mongolian forest steppe (FS_m), and Chinese agro-pastoral transition zone (A_c). They correspond to areas with distinct ranges of precipitation amount. Note the southward and westward decreasing gradients of P and NDVI over the highlighted area of Mongolia and Chinese Inner Mongolia.

For 1999–2002, negative anomalies of P_{6-8} were widespread not only in Asia, but also in the Northern Hemisphere (not shown). This pattern is similar to that for $NDVI_8$ (Lotsch et al. 2005). Figure 3 displays changes in (a) P_{6-8} , and (b) $NDVI_8$, from 1998 (pre-drought year) to 1999 (drought year), and those (d and e) from 2002 (drought year) to 2003 (post-drought year). P_{6-8} and $NDVI_8$ decreased simultaneously over an extensive area between 1998 and 1999 (Fig. 3a, b), whereas similar patterns of opposite sign are evident in the change from 2002 to 2003 (Fig. 3d, e). Indices of sensitivity (SI) and resilience (RI) of vegetation to drought during 1999–2002 are presented in Fig. 3c, f, respectively. Areas without consistent signs (positive in panels a and b vs. negative in d and e) for change in precipitation and vegetation are denoted by blank areas, and excluded in the following analysis. Higher values of RI were observed over the driest area straddling the boundary of Mongolia and China, whereas SI values were relatively even across the area.

Figure 4 shows interannual variations of P_{6-8} and $NDVI_8$ for the five sub-regions. The two parameters in the

Table 1 Regionally averaged climatological P_{ann} , P_{6-8} , interannual maximum and minimum P_{6-8} ; climatological NDVI₈, interannual maximum and minimum NDVI₈; aridity index (AI) (UNEP 1992);

indices of sensitivity (SI) and resilience (RI); regional averages of SI and RI (AVE), regionally adjusted SI ($SI/AVE: SI_r$); and RI ($RI/AVE: RI_r$) for the five sub-regions

Sub-regions	Clim. P_{ann}	Clim. P_{6-8}	Max. P_{6-8}	Min. P_{6-8}	Clim. NDVI ₈	Max. NDVI ₈	
Desert steppe (DS_m)	130	93	167	39	0.11	0.20	
Mongolian steppe (S_m)	216	153	266	75	0.30	0.41	
Chinese steppe (S_c)	233	159	250	81	0.30	0.39	
Mongolian forest steppe (FS_m)	290	199	400	111	0.47	0.57	
Chinese cultivated land (C_c)	359	265	385	156	0.49	0.59	
Sub-regions	Min. NDVI ₈	AI	SI	RI	AVE	SI_r (SI/AVE)	RI_r (RI/AVE)
Desert steppe (DS_m)	0.08	0.13	0.25	1.40	0.62	0.40	2.26
Mongolian steppe (S_m)	0.22	0.15	0.31	0.93	0.44	0.70	2.11
Chinese steppe (S_c)	0.23	0.25	0.11	2.65	0.25	0.44	10.60
Mongolian forest steppe (FS_m)	0.38	0.24	0.41	0.50	0.20	2.05	2.50
Chinese cultivated land (C_c)	0.38	0.44	0.15	0.31	0.13	1.15	2.38

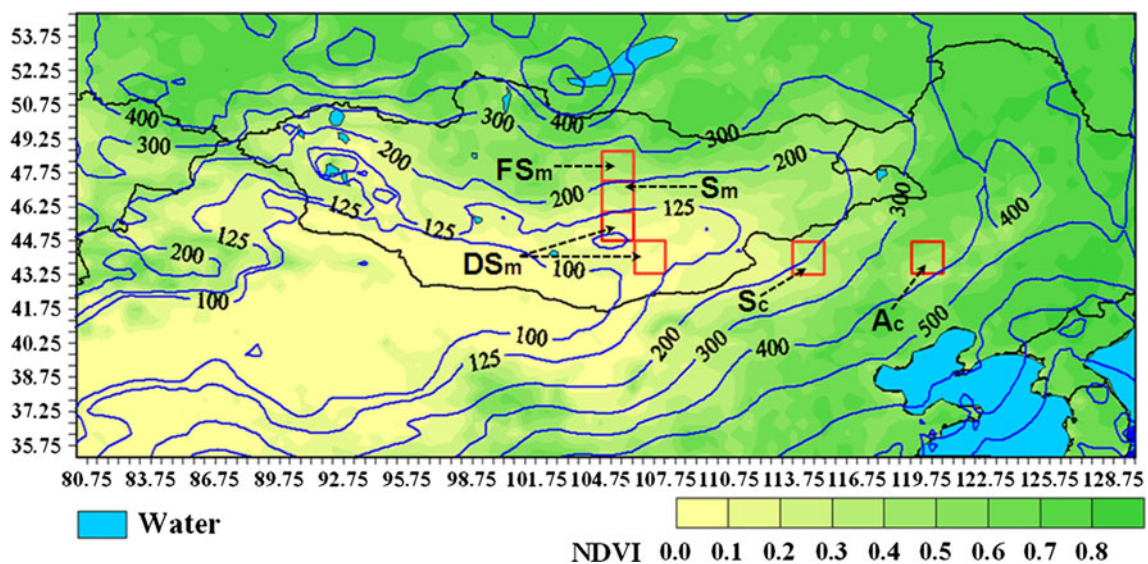


Fig. 2 Annual mean precipitation (P , mm) and NDVI for August (1981–2009) across study area and five sub-regions (square areas bounded by red lines) along cross sections 104.75–106.25°E and 43.25–45.75°N: desert steppe (DS_m), Mongolian (S_m) and Chinese (S_c) steppes, Mongolian forest steppe (FS_m), and Chinese agro-

pastoral region (A_c). Precipitation and vegetation data were averaged over grid points in sub-regions to derive regional average values. Areas with normal response of decreased and increased NDVI corresponding to decreased and increased P were used for sub-region selection

Mongolian regions are significantly correlated ($p = 0.05$), exhibiting consistent changes of the same sign from 1998 to 1999 and 2002 to 2003. On the other hand, the parameters for the Chinese regions are not significantly correlated, probably owing to anthropogenic influences as explained below. Figure 5 depicts relationships between P_{6-8} and NDVI₈. Slopes of the red and blue arrows denote responses of NDVI₈ to P_{6-8} from 1998 to 1999 and 2002 to 2003, respectively. In general, the amplitude of resilience (blue) is much larger than that of sensitivity (red) across the desert steppe and steppe regions (DS_m , S_m , and S_c), whereas

they appear to have similar (and small) amplitude across the wetter regions (FS_m and A_c).

Figure 6 illustrates relationships between P_{6-8}/P_{m6-8} and NDVI₈/NDVI_{m8}. As explained in “Formulating sensitivity and resiliency indices” section, the P_{6-8} and NDVI₈ values were normalized by respective values averaged over the entire period of 1981–2009 (climatology). Slopes of the red and blue arrows for each region, which designate changes from 1998 to 1999 and 2002 to 2003, respectively, correspond to the respective SIs and RI s (Table 1). In general, the amplitude of RI is much larger than that of SI

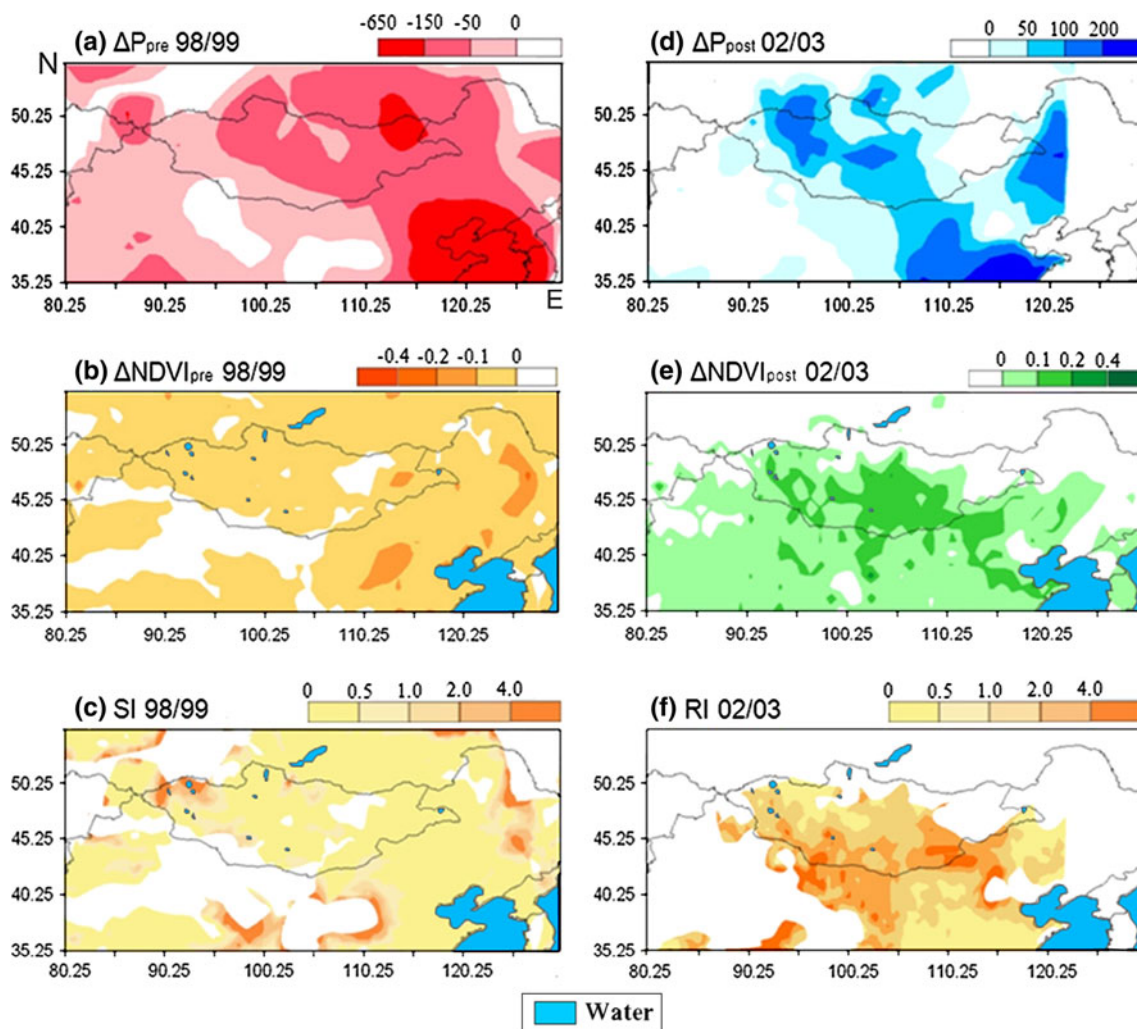


Fig. 3 Changes in **a** P_{6-8} (mm), and **b** $NDVI_8$ from 1998 (pre-drought year) to 1999 (drought year), and those (**d**, **e**) from 2002 (drought year) to 2003 (post-drought year). Also shown are indices of **c** sensitivity (SI), and **f** resilience RI of vegetation to drought during

2000–2002. Blank areas in **c** and **d** were excluded in the analysis because they did not have consistent changes of P_{6-8} and $NDVI_8$ (i.e., $SI < 0$ or $RI < 0$)

across the desert steppe and steppe regions (DS_m , S_m , and S_c), whereas they appear to have similar, small amplitudes across the wetter regions (FS_m and A_c).

Figure 7 portrays relationships between dP_{6-8}/P_{m6-8} and $dNDVI_8/NDVI_{m8}$. A slope connecting the point of origin with each point is regarded as RI in the first quadrant and SI in the third quadrant. The red and blue dots denote values for 1999 and 2003, respectively; absolute value of the slope is higher for RI than for SI (Table 1), as seen in the diagrams of different scales (Fig. 6). The two parameters related to dP_{6-8} and $dNDVI_8$ in Fig. 7 reveal more significant correlations than those in Fig. 6. This indicates that the state of vegetation in the previous year somewhat affects that of the current year. This implies that vegetation memory is maintained from the previous year and affects the state of the current year (Nandintsetseg et al. 2010).

As explained in “Formulating sensitivity and resiliency indices” section, regionally adjusted indices of sensitivity (SI_r) and resilience (RI_r) of vegetation to drought were used to do an interregional comparison of interannual vegetation dynamics. In terms of the new indices (Table 1), the amplitude of resilience (RI_r) is generally larger than that of sensitivity (SI_r) across all regions, whereas they have similar amplitudes across the wetter regions (FS_m and A_c). Furthermore, a vulnerability analysis using SI and RI vectors (“Vulnerability and instability analyses” section) identified non-resilient areas, where composited vectors of $R + S$ indicated decreased vegetation despite increased precipitation during the post-drought year (indicated by red vectors in Fig. 8). These areas were on the south side of the Khangai Mountains in western Mongolia (Area 1 in Fig. 8), near the A_c area (Area 2), and on the Loess Plateau, especially the Ordos Plateau (Area 3). Highly resilient

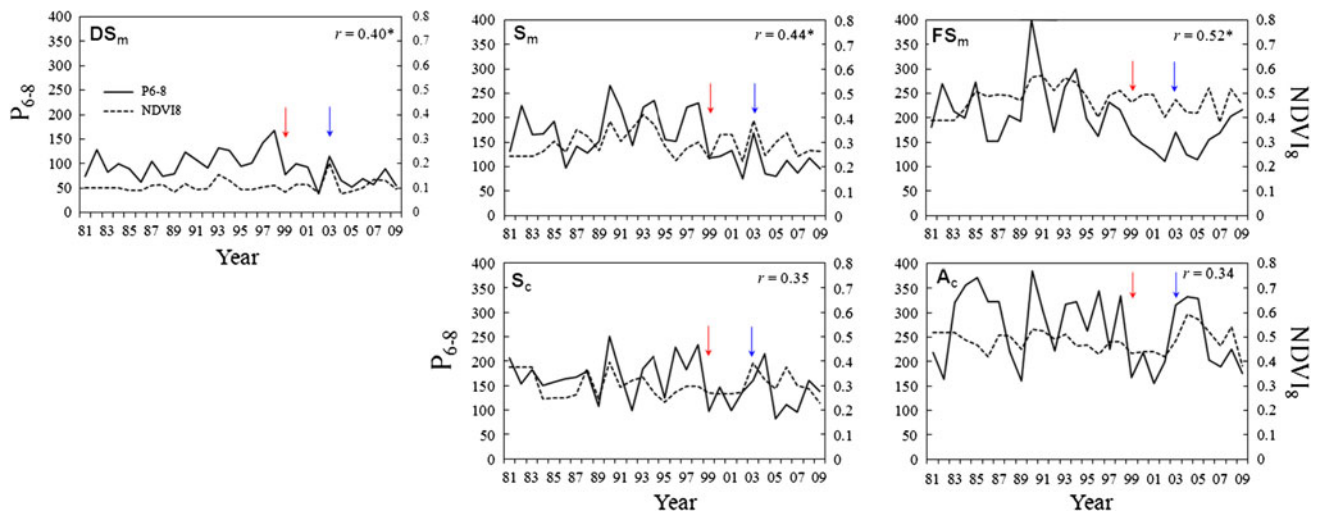


Fig. 4 Interannual variations of P_{6-8} (mm) and $NDVI_8$ for the five sub-regions during 1981–2009. Arrows denote timing of changes from 1998 to 1999 and 2002 to 2003. Asterisks following correlation coefficient denote 5 % significance level

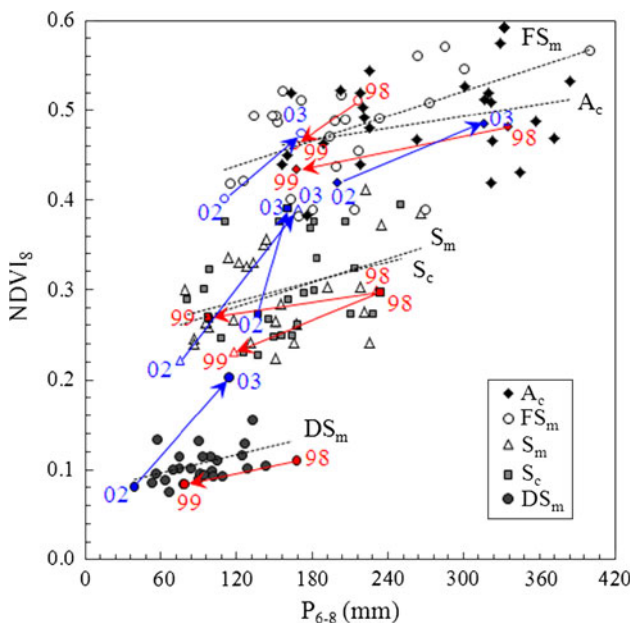


Fig. 5 Relationships between P_{6-8} (mm) and $NDVI_8$ for the five sub-regions during 1981–2009. Varying symbols represent different regions. Red and blue arrows denote changes from 1998 to 1999 and 2002 to 2003 for each region, respectively. Dashed lines are those of linear regression for each region

areas, where the $R + S$ vectors indicated increased vegetation despite decreased precipitation in the post-drought year (indicated by blue vectors), were widely observed across the steppe area from S_m to S_c . Even for ecosystems in areas regarded as non-resilient or of low resilience, there is a memory mechanism whereby multiyear drought was followed by delayed recovery of vegetation during post-drought years, as observed on the Mongolian steppe (Nandintsetseg et al. 2010).

We have investigated the persistence of interannual anomalies of soil moisture and vegetation produced by summer drought (below-normal P) (Shinoda and Nandintsetseg 2011; Nandintsetseg and Shinoda 2012). These anomalies tend to be maintained from summer through spring because of the cold winter climate, but to be interrupted by external forcing in the following early summer. Also, the DREX documented rapid resilience of AGP, based on large BGP (Shinoda et al. 2010). These investigations focused on year-to-year variability of the ecosystem responding to a single-year drought. However, it is unknown how multiyear drought impacts the rootstock that acts as a drought memory, and how this is reflected in the NDVI and proposed indices. If we recall that BGP is several times AGP on the steppe, the rootstock may have a longer memory since it has a greater proportion of total phytomass from the desert steppe to typical and forest steppes and causes a delay in the recovery of AGP (as revealed by the NDVI). This speculation coincides with a slower response of NDVI across the forest steppe, as seen in the resiliency index.

Instability analysis was done on long-term trends of SI and RI (Fig. 9; “Vulnerability and instability analyses” section). The indices for FS_m and A_c revealed significant increasing trends ($p < 0.05$) over the past three decades (especially during the 2000s), implying reduced vegetation stability (or greater instability to climate change) in terms of NDVI. In the forest steppe (FS_m), P_{6-8} varied greatly prior to 1998, whereas $NDVI_8$ remained relatively high, producing small SI and RI values. On the other hand, this stable state of $NDVI_8$ appeared to change into a regime with a relatively variable state during and after the drought of 1999–2002. A possible reason for this is the recently decreased area of forest cover (13.1 % was lost during

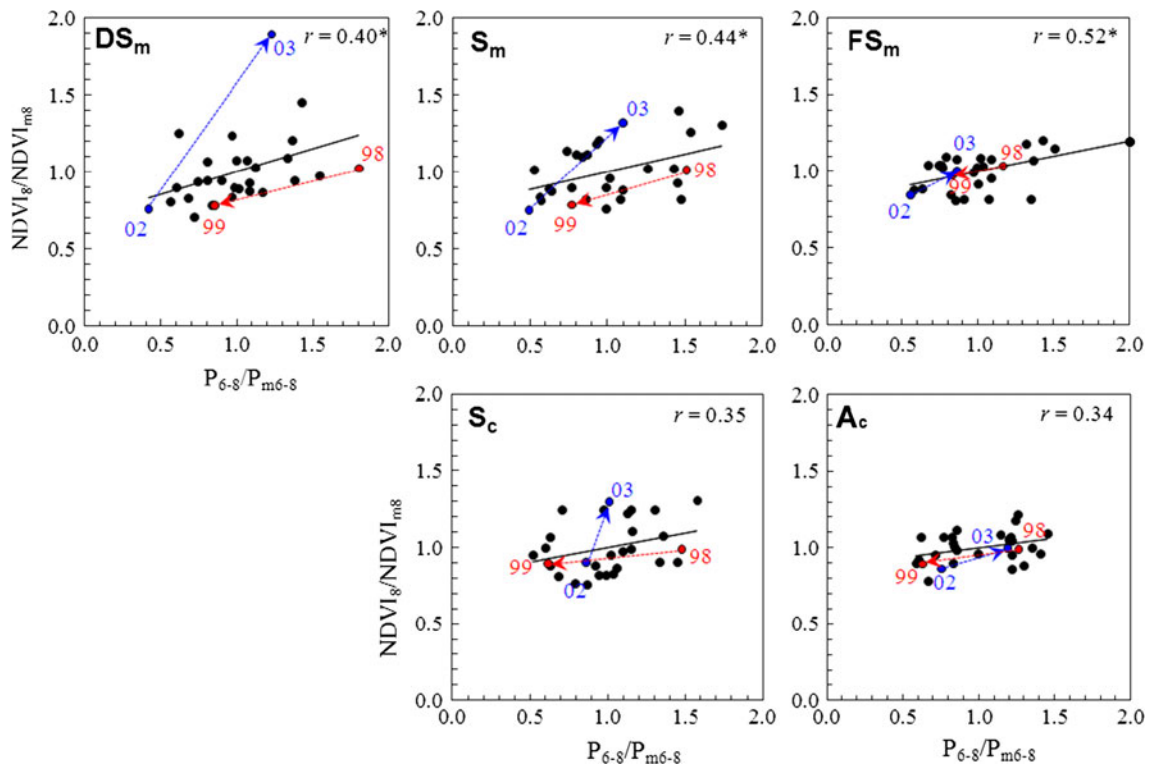


Fig. 6 Correlations between P_{6-8}/P_{m6-8} and $NDVI_{8}/NDVI_{m8}$ for the five sub-regions during 1981–2009. Red and blue arrows depict changes from 1998 to 1999 and 2002 to 2003, respectively. Solid lines are those of linear regression. Asterisks indicate 5 % significance

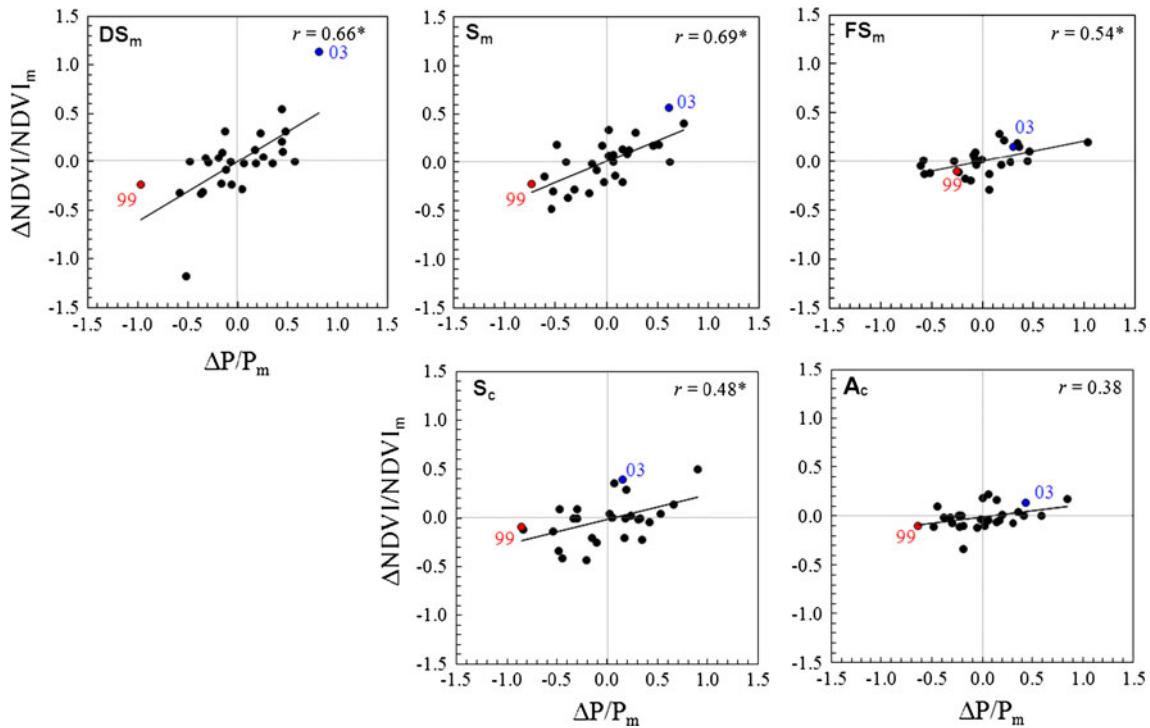


Fig. 7 Relationships between dP_{6-8}/P_{m6-8} and $dNDVI_{8}/NDVI_{m8}$ for the five sub-regions during 1981–2009. Red and blue dots show values for 1999 and 2003, respectively. Solid lines are those of linear regression

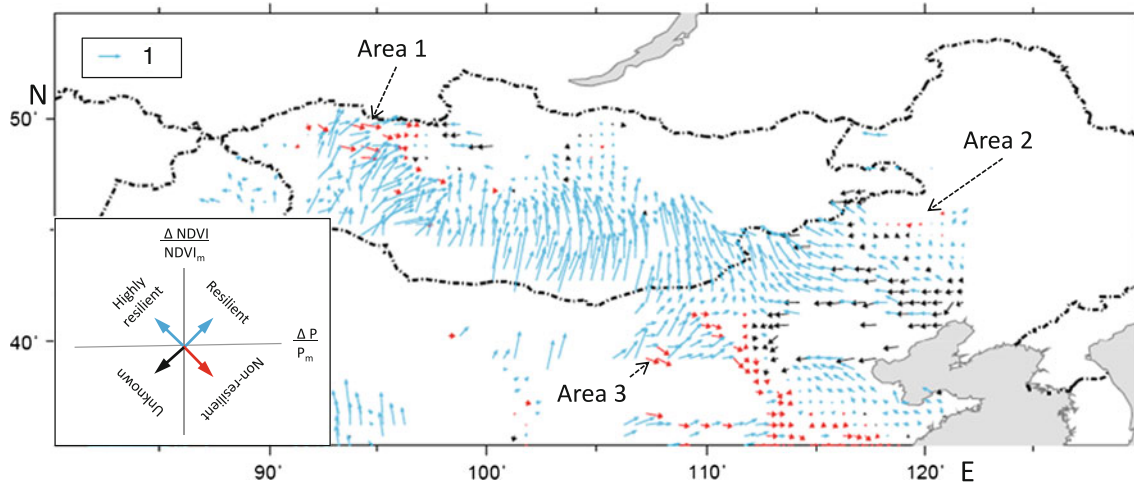


Fig. 8 Spatial pattern of vectors of SI plus RI , that is, $S(dP_{pre}/P_m, dV_{pre}/V_m)$ plus $R(dP_{post}/P_m, dV_{post}/V_m)$. Potentially vulnerable areas are identified by $R + S$ vectors indicating decreased vegetation, in spite of increased precipitation during post-drought year. Highly

resilient areas are identified by $R + S$ vectors indicating increased vegetation, in spite of decreased precipitation during post-drought year

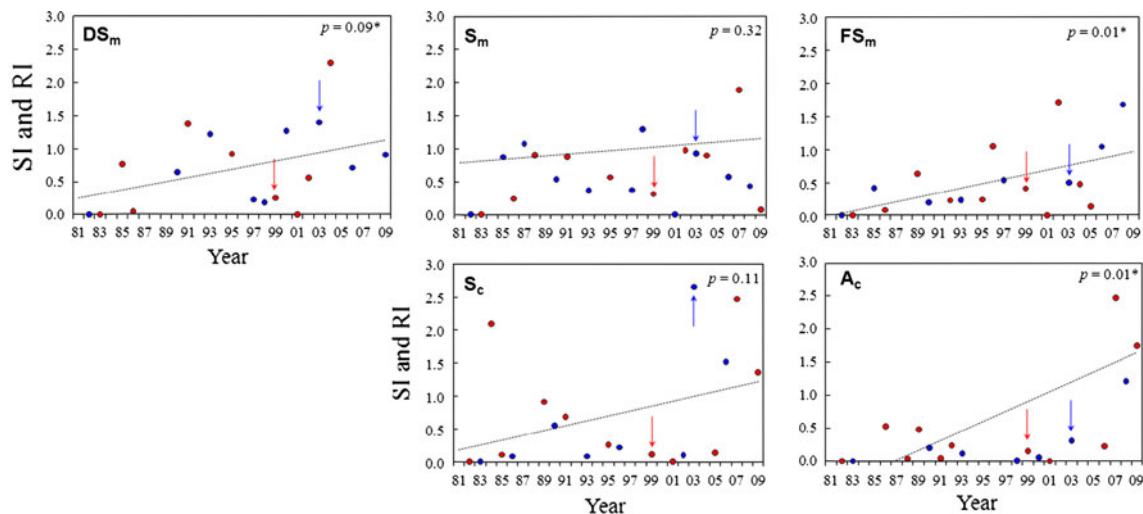


Fig. 9 Interannual variations of SI (red) and RI (blue) for the five sub-regions during 1982–2009. Red and blue arrows represent changes from 1998 to 1999 and 2002 to 2003, respectively. Dashed

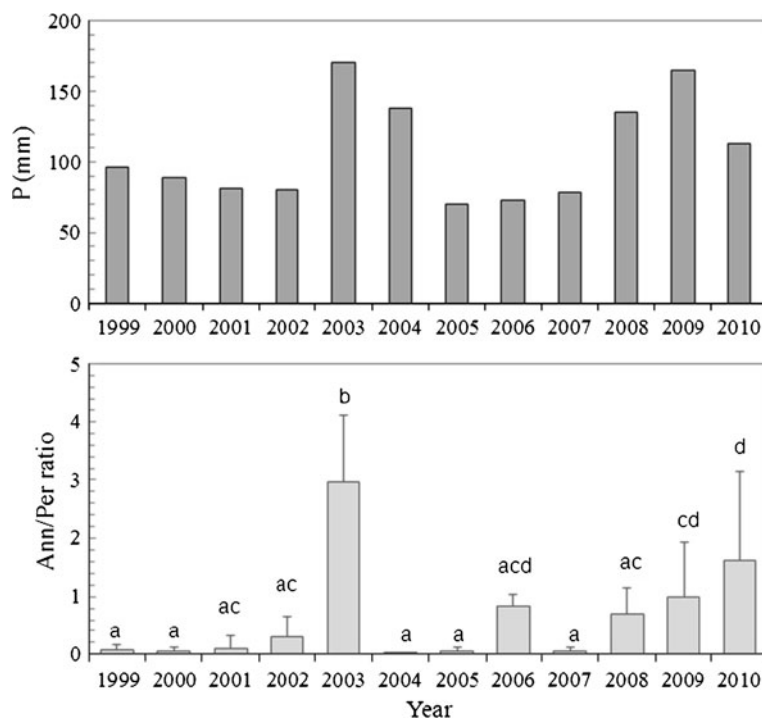
lines show linear regression lines for SI and RI . Asterisks near trend denote 5 % significance level

1990–2010) in northern Mongolia (FAO 2010) and resulting increased proportion of grasses. This generates a state of NDVI (i.e., AGP) that is sensitive to precipitation change. Also, the Chinese agro-pastoral area (A_c) was identified as one with increasingly unstable conditions and low resilience (Fig. 8). Furthermore, the slightly less resilient area north of A_c (Area 2) appears to coincide with that having a dominant decreasing trend of NDVI residual from the rainfall-NDVI regression (i.e., human-induced vegetation degradation) for 1991–2000 (Li et al. 2012). All these findings imply inappropriate management of the land-use system during recent years. This system is largely controlled by human intervention and not just by climatic

variability, as explained later (Fig. 11). On the other hand, we have no clear evidence that supports the conventional view of the transnational pattern of desertification that is more pronounced in eastern Inner Mongolia and Northeast China than in Mongolia (UNEP 1992; Lepers et al. 2005; de Noblet-Ducoudré et al. 2012). One of the major reasons for this discrepancy is that the previous studies used different data sources (some of them were experts' opinions) from the two countries; this is not the case in the present objective analysis.

Figure 10 displays interannual variations of plant-available precipitation as defined by Shinoda et al. (2010) and the ratio of annual to perennial phytomass (Ann/Per)

Fig. 10 Interannual variations of plant-available precipitation (accumulated values from 1 May through earlier dates of phytomass sampling, mm) and ratio of annual to perennial phytomass (Ann/Per) at BU_s site (46°49′47.46″N, 105°47′35.34″E, 1,354 masl) on Mongolian steppe during 1999–2010. Ratios labeled with different letters differ significantly ($p < 0.05$) between years



on the Mongolian steppe. The asymmetric responses of $SI_r < RI_r$ (or $SI < RI$), which were manifested in the desert steppe–steppe regions (Table 1), are likely explained by a change in plant species composition (i.e., a larger Ann/Per ratio for the post-drought year 2003 than for the drought years 1999–2002). This interpretation is supported by an investigation of species composition on the Mongolian steppe (Shinoda et al. 2010), although its data did not fully cover the drought period of interest. The Chinese steppe area had a much higher RI_r than the Mongolian one. This may be because of a larger Ann/Per ratio in species composition, but not significantly because of grazing pressure, which was nearly the same in the two sub-regions before and during the drought (as explained later; Fig. 12). After 2003, the ratio quickly returned to the level prior to the drought years (1999). This indicates a succession process of steppe vegetation after a disturbance such as drought.

Figure 11 depicts seasonal changes of P and NDVI for 1998 (pre-drought year), 1999–2002 (drought years), and 2003 (post-drought year). In general, for 2003, P more or less recovered from its level in the drought years (1999–2002), although it did not reach the pre-drought level of 1998. For the desert steppe (DS_m) and steppe (S_m and S_c), it only reached a level between those of 1998 and 1999–2002. Interestingly, in response to the incomplete recovery of P during 2003, NDVI drastically increased in July, exceeding the level of 1998; this was manifested in DS_m , S_m , and S_c . There was a similar NDVI response to increased P in FS_m . This increased NDVI during the early rainy season (July) is likely attributable to similarly

increased annual species (increased Ann/Per ratio) that were clearly observed at site BU_s in S_m (Fig. 10). This is the nature of such species, which respond more quickly to rainy season onset after a multiyear drought. However, similar seasonal courses of NDVI in A_c between the drought and non-drought years may have resulted from improved land-use management strategies (e.g., irrigation and afforestation) that are not very subject to climatic variability.

Figure 12 indicates that in general, livestock density was nearly identical in both steppe regions (S_c and S_m), except in the late 2000s. On a larger spatial scale, the density had an increasing trend over the past several decades in Mongolia (Sugita et al. 2007; Komiyama and Chantsaldulam 2011) and Chinese Inner Mongolia (Li et al. 2011). The density declined dramatically in 2000 and turned into an increase around 2003. Afterward, the increasing tendency strengthened in Mongolia. There, the decreased density during 2000–2003 was caused by harsh cold-season weather (*dzud* in Mongolian) during the three seasons from 1999–2000 to 2001–2002 following summer droughts (e.g., Tachiiri et al. 2008; Begzsuren et al. 2004). It is believed that similar weather conditions resulted in livestock mortality in China during the 1999–2000 cold season. Synoptic analysis showed that in this winter, relatively cold atmospheric anomalies covered eastern Inner Mongolia (not shown). Subsequently, livestock density in S_c decreased slightly during the late 2000s, owing to the introduction of projects to restore grasslands by grazing prohibition, zoning rotation grazing, and fencing (Li et al.

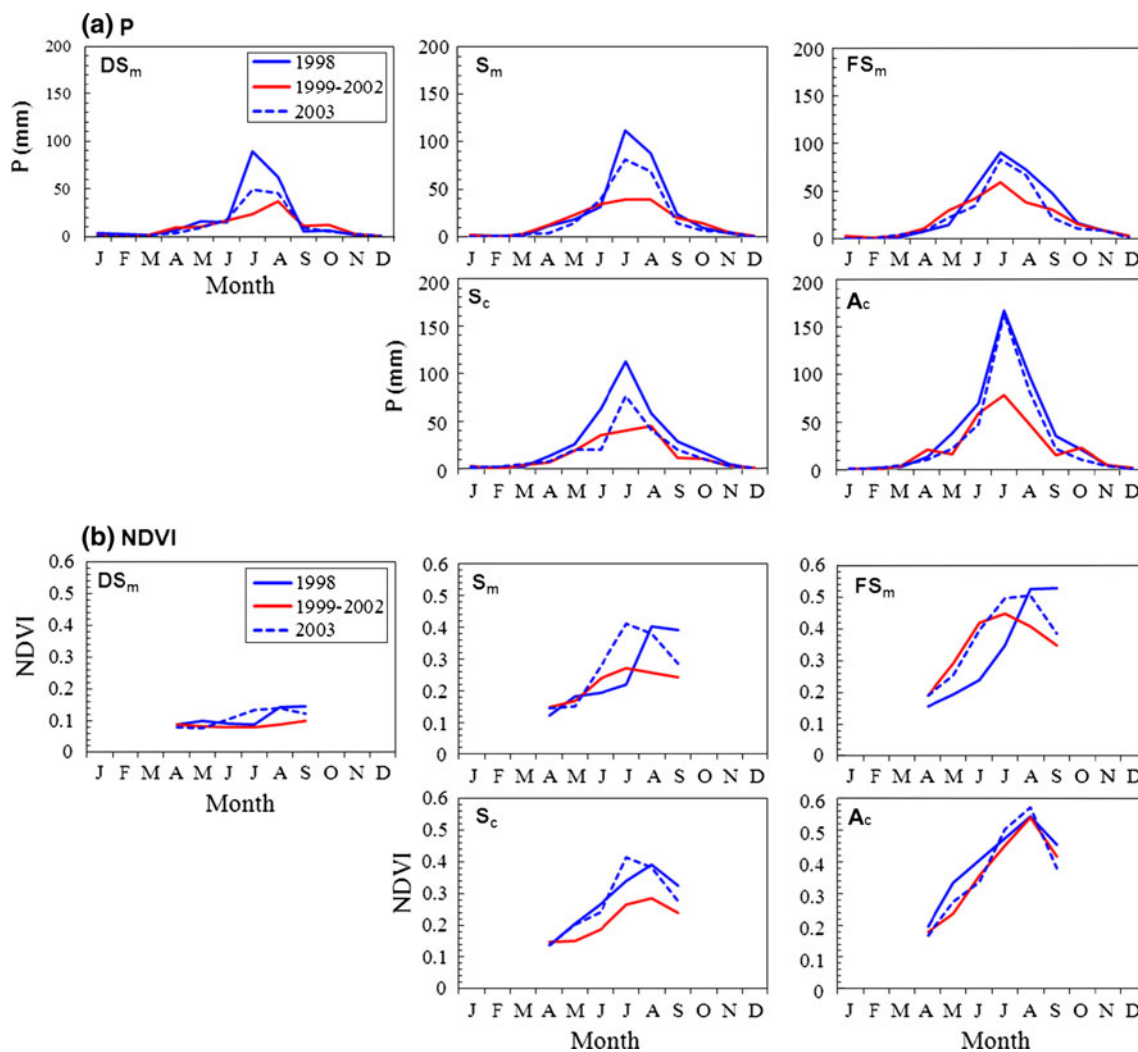


Fig. 11 Seasonal changes of **a** P (mm), and **b** NDVI of the five sub-regions for 1998 (pre-drought year, blue curves), 1999–2002 (drought years, red curves), and 2003 (post-drought year, dashed blue curves)

2011). The greatly reduced livestock number in Mongolia and Inner Mongolia during the early 2000s most likely caused similarly reduced grazing pressure, ultimately strengthening the resilience of pasture conditions. This is one plausible explanation for $SI_r < RI_r$, in addition to the vegetation dynamics itself with increased Ann/Per ratio.

Conclusions

The multiyear drought highlighted here, which was the severest on the continental scale over the past three decades, provided a unique experimental opportunity in an earth laboratory to explore drought impact on the terrestrial ecosystem. This novel approach quantified the sensitivity and resilience of vegetation to drought on the continental scale. We developed new sensitivity and resiliency indices in this context and showed that these indices have

implications for vegetation dynamics in the response. We demonstrated that the vegetation dynamics depend on drought phase (initial or ending), vegetation type, land-use management (pasturing or cropping), and extent of land degradation.

The newly proposed indices were used to evaluate ecosystem vulnerability and instability and to identify locations where resilience of vegetation conditions affected by drought was not observed (i.e., vegetation was non-resilient) in spite of increased precipitation, and/or where long-term stability of vegetation was under threat. The results show non-resilient areas on the south side of the Khangai Mountains in western Mongolia, near the Chinese agro-pastoral region, and on the Loess Plateau, especially the Ordos Plateau; vegetation stability was under threat in the forest steppe and agro-pastoral region over the past three decades. However, the results do not support the conventional view of a transnational desertification pattern

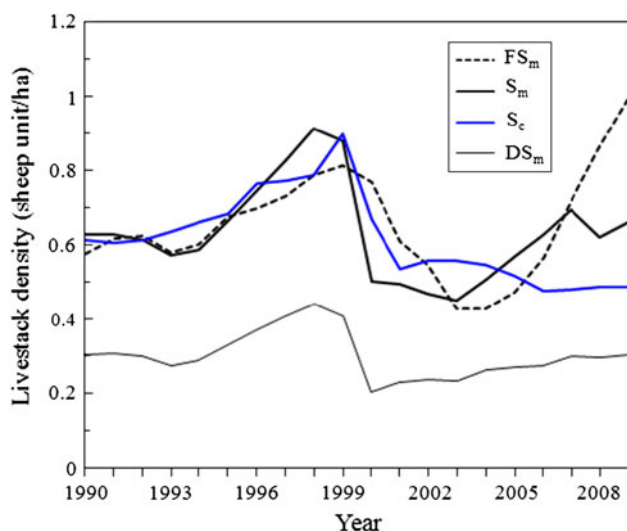


Fig. 12 Interannual variations of livestock density (sheep unit/ha) in sub-regions (except for Chinese agro-pastoral region A_c) during 1990–2009

that is more pronounced (probably from human impacts) in eastern Inner Mongolia and Northeast China than in Mongolia.

In short, we proposed a method to identify a vulnerable location, using two types of analyses of vectors and long-term trends of the sensitivity and resiliency indices. Detailed field surveys of these areas are expected to verify the regional resilience suggested by our large-scale analysis. In future study, this method will help provide early warning of desertification that may emerge as a non-resilient regime shift, from vegetated to degraded (or desertified) surface. Moreover, future investigation should attempt to apply the method to other regions where the ecosystem is under threat, and to extend it to socioeconomic phenomena.

Acknowledgments We thank Dr. Y. Cheng for her useful advice on vegetation dynamics and land use in the study area. Thanks also go to Dr. T. Bat-Oyun for analysis of the phytomass data and to Dr. T. Koike for analysis of the synoptic data. This research was supported by Grants-in-Aid for Scientific Research and the Japan Society for the Promotion of Science (JSPS) Fellows (Nos. 16405002, 20255001, and 22-00399).

Open Access This article is distributed under the terms of the Creative Commons Attribution License which permits any use, distribution, and reproduction in any medium, provided the original author(s) and the source are credited.

References

Bai Y, Han X, Wu J, Chen Z, Li L (2004) Ecosystem stability and compensatory effects in the Inner Mongolia grassland. *Nature* 431:181–183

- Bayarjargal Y, Karnieli A, Bayasgalan M, Khudulmur S, Gandush C, Tucker CJ (2006) A comparative study of NOAA–AVHRR derived drought indices using change vector analysis. *Remote Sens Environ* 105(1):9–22
- Begzsuren S, Ellis JE, Ojima DS, Coughenour MB, Chuluun T (2004) Livestock responses to droughts and severe winter weather in the Gobi Three Beauty National Park. *J Arid Environ* 59:785–796
- Brown ME, Pinzón JE, Didan K, Morisette JT, Tucker CJ (2006) Evaluation of the consistency of long-term NDVI time series derived from AVHRR, SPOT-vegetation, SeaWiFS, MODIS, and Landsat ETM+ sensors. *IEEE Trans Geosci Remote Sens* 44:1787–1793
- Charney JG, Arakawa A, Baker DJ, Bolin B, Dickinson RE, Goody RM, Leith CE, Stommel HM, Wunsch CI (1979) Carbon dioxide and climate: a scientific assessment. National Academy of Sciences, Washington, DC, p 22
- Chen WY, Xiao QG, Sheng YW (1994) Application of the anomaly vegetation index to monitoring heavy drought in 1992 (in Chinese). *China Remote Sens Environ* 9:106–112
- Cheng Y, Tsubo M, Ito T, Nishihara E, Shinoda M (2011) Impact of rainfall variability on plant diversity in grazing land: a case study from Mongolia. *J Arid Environ* 75(5):471–476
- China Vegetation Atlas Editorial Committee of the Chinese Academy of Science (2001) Atlas China vegetation (in Chinese). Science Press, Beijing
- Chuai XW, Huang XJ, Wang WJ, Bao G (2012) NDVI, temperature and precipitation changes and their relationships with different vegetation types during 1998–2007 in Inner Mongolia, China. *Int J Climatol*. doi:10.1002/joc.3543
- Clark WC, Dickson NM (2003) Sustainability science: the emerging research program. *Proc Natl Acad Sci USA* 100(14):8059–8061
- Dai A, Trenberth KE, Qian T (2004) A global data set of Palmer drought severity index for 1870–2002: relationship with soil moisture and effects of surface warming. *J Hydrometeorol* 5:1117–1130
- De Noblet-Ducoudré N, Boissier JP, Pitman A, Bonan GB, Brovkin V, Cruz F, Delire C, Gayler V, van den Hurk BJM, Lawrence PJ, van der Molen MK, Müller C, Reick CH, Strengers BJ, Voldoire A (2012) Determining robust impacts of land-use-induced land cover changes on surface climate over North America and Eurasia: results from the first set of LUCID experiments. *J Clim* 25:3261–3281
- Fernandez-Gimenez ME, Allen-Diaz B (1999) Testing a non-equilibrium model of rangeland vegetation dynamics in Mongolia. *J Appl Ecol* 36:871–885
- Fernandez-Gimenez ME, Allen-Diaz B (2001) Vegetation change along gradients from water sources in three grazed Mongolian ecosystems. *Plant Ecol* 157:101–118
- Food and Agriculture Organization of the United Nations (FAO) (2010) Main report on global forest resources assessment 2010. FAO, Rome
- Füssel HM (2007) Vulnerability: a generally applicable conceptual framework for climate change research. *Glob Environ Chang* 17:155–167
- Gao YZ, Giese AM, Han AXG, Wang ADL, Zhou ZY, Brueck AH, Lin AS, Taube AF (2009) Land use and drought interactively affect interspecific competition and species diversity at the local scale in a semiarid steppe ecosystem. *Ecol Res* 24:627–635
- Guha-Sapir D, Hargitt D, Hoyois P (2004) Thirty years of natural disasters 1974–2003: the numbers. Presses Universitaires de Louvain, Louvain-la-Neuve, Belgium
- Hartvigsen G (2000) Competition between co-dominant plants of the Serengeti plains depends on competitor identity, water, and urine. *Plant Ecol* 148:31–41
- Hooper DU, Adair EC, Cardinale BJ, Byrnes JEK, Hungate BA, Matulich KL, Gonzalez A, Duffy JE, Gamfeldt L, O'Connor MI

- (2012) A global synthesis reveals biodiversity loss as a major driver of ecosystem change. *Nature* 486:105–108. doi:10.1038/nature11118
- Huxman TE, Smith MD, Fay PA, Knapp AK, Shaw MR, Loik ME, Smith SD, Tissue DT, Zak JC, Weltzin JK, Pockman WT, Sala OE, Haddad BM, Harte J, Koch GW, Schwinning S, Small EE, Williams DG (2004) Convergence across biomes to a common rain-use efficiency. *Nature* 429:651–654
- IPCC (2007) Climate change 2007: mitigation. In: Metz B, Davidson O, Bosch P, Dave R, Meyer L (eds) Contribution of working group III to the fourth assessment report of the intergovernmental panel on climate change. Cambridge University Press, Cambridge
- Iwasaki H (2006) Impact of interannual variability of meteorological parameters on vegetation activity over Mongolia. *J Meteorol Soc Jpn* 84:745–762
- Kates RW, Clark WC, Corell R, Hall JM, Jaeger CC, Lowe I, McCarthy JJ, Schellnhuber HJ, Bolin B, Dickenson NM, Faucheux S, Gallopin GC, Grubler A, Huntley B, Jaeger J, Jodha NS, Kasperson RE, Mabogunje A, Matson P, Mooney H, Moore B III, O'Riordan T, Svedin U (2001) Sustainability science. *Science* 292:641–642
- Komiya H, Chantsaldulam R (2011) Changes of animal husbandry and crop farming in Mongolia during past half a century and the future perspective. *J Arid Land Stud* 21(1):37–43
- Kondoh A, Kaihotsu I, Hirata M, Azzaya D (2005) Interannual variation of phenology and biomass in Mongolian herbaceous vegetation. *J Arid Land Stud* 14:209–218 (in Japanese with English abstract)
- Lepers E, Lambin EF, Janetos AC, DeFries R, Achard F, Ramankutty N, Scholes RJ (2005) A synthesis of rapid land-cover change information for the 1981–2000 period. *Bioscience* 55(2):115–124
- Li Y, Du F, Muyuan (2011) Protecting grassland ecological and promoting the sustainable development of Inner Mongolia's animal husbandry. Sustainable development of animal husbandry in Northeast Asia. Inner Mongolia People's Publishing House, pp 42–59
- Li A, Wu J, Huang J (2012) Distinguishing between human-induced and climate-driven vegetation changes: a critical application of RESTREND in Inner Mongolia. *Landsc Ecol* 27:969–982
- Lotsch A, Friedl MA, Anderson BT, Tucker CJ (2005) Response of terrestrial ecosystems to recent northern hemispheric drought. *Geophys Res Lett* 32:L06705. doi:10.1029/2004GL022043
- Ma ZG, Fu CB (2003) Interannual characteristics of the surface hydrological variables over the arid and semi-arid areas of northern China. *Glob Planet Chang* 37:189–200
- Milchunas DG, Lauenroth WK, Chapman PL, Kazempour MK (1989) Effects of grazing, topography, and precipitation on the structure of a semi-arid grassland. *Vegetation* 80:11–23
- Mitchell TD, Jones PD (2005) An improved method of constructing a database of monthly climate observations and associated high-resolution grids. *Int J Climatol* 25(6):693–712. doi:10.1002/joc.1181
- Miyazaki S, Yasunari T, Miyamoto T, Kaihotsu I, Davaa G, Oyunbaatar D, Natsagdorj L, Oki T (2004) Agrometeorological conditions of grassland vegetation in central Mongolia and their impact for leaf area growth. *J Geophys Res* 109:D22106. doi:10.1029/2004JD005658
- Munkhtsetseg E, Kimura R, Wang J, Shinoda M (2007) Pasture yield response to precipitation and high temperature in Mongolia. *J Arid Environ* 70:94–110
- Nachinshonhor UG (2012) Use of steppe vegetation by nomadic pastoralists in Mongolia. In: Yamamura N, Fujita N, Maekawa A (eds) The Mongolian ecosystem network. Environmental issues under climate and social changes, ecological research monographs. Springer, Tokyo, pp 147–158
- Nandintsetseg B, Shinoda M (2012) Multi-decadal soil moisture trends and their relationship to precipitation and evapotranspiration over three vegetation zones in Mongolia. *Arid Land Res Manag* (under review)
- Nandintsetseg B, Shinoda M (2013) Assessment of drought frequency, duration, and severity, and its impact on pasture production in Mongolia. *Nat Hazards* 66:995–1008
- Nandintsetseg B, Shinoda M, Kimura R, Ibaraki Y (2010) Relationship between soil moisture and vegetation activity in the Mongolian steppe. *SOLA* 6:032–062
- NASA Land Processes Distributed Active Archive Center (LP DAAC) (2012) Vegetation indices 16-day L3 global 0.05 deg CMG. USGS/Earth Resources Observation and Science (EROS) Center, Sioux Falls. http://lpdaac.usgs.gov/get_data. Accessed 20 June 2012
- Natsagdorj L (2003) Climate change. In: Batima P (ed) Climate change: pasture and animal husbandry. Institute of Meteorology and Hydrology of Mongolia, Ulaanbaatar, pp 13–14
- Nemani RR, Keeling CD, Hashimoto H, Jolly WM, Piper SC, Tucker CJ, Myneni RB, Running SW (2003) Climate-driven increases in global terrestrial net primary production from 1982 to 1999. *Science* 300:1560–1563
- Obasi GOP (1994) WMO's role in the international decade for natural disaster reduction. *Bull Am Meteorol Soc* 75:1655–1661
- Pinzon J (2002) Using HHT to successfully uncouple seasonal and interannual components in remotely sensed data. In: Proceedings of the SCI 2002 conference, July 14–18, Orlando, FL
- Sasaki T, Okayasu T, Ohkuro T, Shirato Y, Jamsran U, Takeuchi K (2009) Rainfall variability may modify the effects of long-term enclosure on vegetation in Mandalgobi, Mongolia. *J Arid Environ* 73:949–954
- Schneider SH, Dickinson RE (1974) Climate modeling. *Rev Geophys Space Phys* 12(3):447–493
- Shinoda M, Nandintsetseg B (2011) Soil moisture and vegetation memories in a cold, arid climate. *Glob Planet Chang* 79(1–2): 110–117
- Shinoda M, Ito S, Nachinshonhor GU, Erdenetsetseg D (2007) Phenology of Mongolian grasslands and moisture conditions. *J Meteorol Soc Jpn* 85:359–367
- Shinoda M, Nachinshonhor GU, Nemoto M (2010) Impact of drought on vegetation dynamics of the Mongolian steppe: a field experiment. *J Arid Environ* 74(1):63–69
- Sugita M, Asanuma J, Tsujimura M, Mariko S, Lu M, Kimura F, Azzaya D, Adyasuren TS (2007) An overview of the rangelands atmosphere–hydrosphere–biosphere interaction study experiment in northeastern Asia (RAISE). *J Hydrol* 333:3–20
- Tachiiri K, Shinoda M, Klinkenberg B, Morinaga Y (2008) Assessing Mongolian snow disaster risk using livestock and satellite data. *J Arid Environ* 72(12):2251–2263
- Tilman D, Downing JA (1994) Biodiversity and stability in grasslands. *Nature* 367:363–365
- Tucker CJ, Pinzon JE, Brown ME, Slayback D, Pak E, Mahoney R, Vermote E, El Saleous N (2005) An extended AVHRR 8-km NDVI data set compatible with MODIS and SPOT vegetation NDVI data. *Int J Remote Sens* 26(20):4485–4498
- Turner BLII, Kasperson RE, Matson PA, McCarthy JJ, Correll RW, Christensen L, Eckley N, Kasperson JX, Luers A, Martello ML, Polsky C, Pulsipher A, Schiller A (2003) A framework for vulnerability analysis in sustainability science. *Proc Natl Acad Sci USA* 100:8074–8079
- UNEP (1992) World atlas of desertification. Arnold, London, p 69
- University of East Anglia Climatic Research Unit (CRU) (2012) CRU time series (TS) high resolution gridded datasets. http://badc.nerc.ac.uk/view/badc.nerc.ac.uk__ATOM__dataent_125622377_3328276. Accessed 20 June 2011

- Vicente-Serrano SM, Gouveia C, Julio Camarero J, Beguería S, Trigo R, López-Moreno JJ, Azorín-Molina C, Pasho E, Lorenzo-Lacruz J, Revuelto J, Morán-Tejeda E, Sanchez-Lorenz A (2012) Response of vegetation to drought time-scales across global land biomes. *Proc Natl Acad Sci USA (PNAS)* 110:52–57
- Wang ZW, Zhai PM (2003) Variation of drought over northern China during 1950–2000. *J Geogr Sci* 13(4):480–487
- Wang P, Wan Z, Li X (2002) Using MODIS land surface temperature and normalized difference vegetation index products for monitoring drought in the Southern Great Plains, USA. In: José AS (ed) *Recent advances in quantitative remote sensing*. Guada Impresors SL, Spain, pp 664–670
- Wesche K, Ronnenberg K, Retzer V, Miehe G (2010) Effects of large herbivore exclusion on southern Mongolian desert steppes. *Acta Oecol* 36:234–241
- Wilhite DA (2000) Drought as a natural hazard: concepts and definitions. In: Wilhite DA (ed) *Drought, a global assessment*, vol 1. Routledge, London, pp 3–18
- Yunatov AA (1976) *Fundamental characteristics of the vegetation of Mongolian People's Republic*. Mongolian Academy of Science, Ulaanbaatar (in Mongolian)
- Zhang Y, Munkhtsetseg E, Kadota T, Ohata T (2005) An observational study of ecohydrology of a sparse grassland at the edge of the Eurasian cryosphere in Mongolia. *J Geophys Res* 110: D14103. doi:[10.1029/2004JD005474](https://doi.org/10.1029/2004JD005474)
- Zou XK, Zhai PM, Zhang Q (2005) Variations in droughts over China: 1951–2003. *Geophys Res Lett* 32:L04707. doi:[10.1029/2004GL021853](https://doi.org/10.1029/2004GL021853)